Structural Engineering and Mechanics, Vol. 39, No. 1 (2011) 147-168
DOI: http://dx.doi.org/10.12989/sem.2011.39.1.147

Capacity design by developed pole placement structural control

Fereidoun Amini* and Kaveh Karami[a]

Department of Civil Engineering, Iran University of Science and Technology, Narmak 16846, Tehran, Iran

(Received September 8, 2009, Accepted April 17, 2011)

Abstract. To ensure safety and long term performance, structural control has rapidly matured over the past decade into a viable means of limiting structural responses to strong winds and earthquakes. Nonlinear response history analysis requires rigorous procedure to compute seismic demands. Therefore the simplified nonlinear analysis procedures are useful to determine performance of the structure. In this investigation, application of improved capacity demand diagram method in the control of structural system is presented for the first time. Developed pole assignment method (DPAM) in structural systems control is introduced. Genetic algorithm (GA) is employed as an optimization tool for minimizing a target function that defines values of coefficient matrices providing the placement of actuators and optimal control forces. The ground acceleration is modified under induced control forces. Due to this, performance of structure based on improved nonlinear demand diagram is selected to threshold of nonlinear behavior of structure. With small energy consumption characteristics, semi-active devices are especially attractive solutions for limiting earthquake effects. To illustrate the efficiency of DPAM, a 30-story steel moment frame structure employing the semi-active control devices is applied. In comparison to the widely used linear quadratic regulation (LQR), the DPAM controller was shown to be just as effective and better in the reduction of structural responses during large earthquakes.

Keywords: developed pole assignment method (DPAM); semi-active optimal control; genetic algorithm (GA); capacity-demand diagram; nonlinear behavior; decreased ground acceleration; linear quadratic regulation (LQR)

1. Introduction

Design and assessment for seismic resistance structures has been undergoing a critical reappraisal in recent years, with the emphasis changing from strength to performance. Performance based seismic engineering (PBSE) is one of the major developments over the past decade, which has been increased attention on limit states. The definition of the philosophy of PBSE is to design a structural system able to sustain a predefined level of damage under a predefined level of earthquake intensity, or, in assessment terms, to identify the damage level of a structure under a predefined earthquake intensity level. It is generally agreed that deformations are more critical parameters for defining performance and as a result it is argued that seismic design and assessment methods should largely

*Corresponding author, Professor, E-mail: famini@iust.ac.ir
[a]Ph.D. Student

be based on them (e.g., Casarotti and Pinho 2007).

Estimating seismic demands at high performance levels, such as life safety and collapse prevention, requires explicit consideration of inelastic behavior of the structure. While nonlinear response history analysis is the most rigorous procedure to compute seismic demands, current civil engineering practice prefers to use simplified, nonlinear analysis procedures have been incorporated in the ATC-40 and FEMA-274 documents to determine the displacement demand imposed on a building expected to deform inelastically (e.g., ATC 1996, FEMA 1997). The nonlinear static procedure in these documents is based on the capacity spectrum method (CSM) originally developed by Freeman (e.g., Freeman *et al.* 1975, Freeman 1978). Nonlinear static assessment approaches based on pushover analysis developed over the past two decades, such as the N2 (e.g., Fajfar *et al.* 1997) method, CSM and some improved methods (e.g., Xue 2001, Xue and Chen 2003, Lee *et al.* 2006) among others, constitute the expression of the well established tendency towards PBSE. The seismic demands are computed by nonlinear static analysis of the structure subjected to monotonically increasing lateral forces with an invariant height wise distribution until a predetermined target displacement is reached. Both the force distribution and target displacement are based on the assumption that the response is controlled by the fundamental mode and that the mode shape remains unchanged after the structure yields (e.g., Chopra and Goel 2002). This feature leads to a transparent transformation from a multi degree of freedom (MDOF) to an equivalent single degree of freedom (SDOF) system. The CSM compares the capacity of the structure in the form of a pushover curve with the demands on the structure in the form of a response spectrum. The graphical intersection of the two curves approximates the response of the structure as shown in Fig. 1 (e.g., Freeman 2004). Improved procedures using the well established inelastic response spectrum are developed. The idea of using the inelastic design spectrum was suggested by Bertero and introduced by Reinhorn and Fajfar (e.g., Bertero 1995, Reinhorn and Fajfar 1997). Inelastic demand spectra are determined from a typical smooth elastic design spectrum. The reduction factors, which relate inelastic spectra to the basic elastic spectrum, are consistent with the elastic spectrum (e.g., Fajfar *et al.* 1997).

The inelastic spectra have been used also by Goel and Chopra (e.g., Chopra and Goel 1999). They suggested the improved capacity demand diagram method that gives the deformation value consistent with the selected inelastic design spectrum, while retaining the attraction of graphical implementation of the ATC-40 methods. However, the improved procedures differ from ATC-40

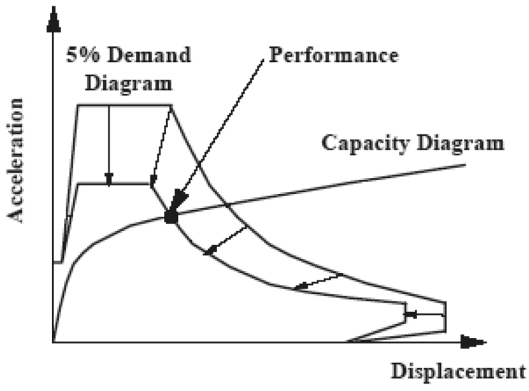

Fig. 1 Graphical determination of structure performance based on Capacity Spectrum Method

procedures in one important sense. The demand is determined by analyzing an inelastic system in the improved procedure instead of equivalent linear systems in ATC-40 procedures.

In recent years optimal control of structures is the main target to minimize energy usage of the control system, during of the induced earthquake (e.g., Amini and Vahdani 2008). Active control systems are expensive to operate due to their high power demands. To overcome these limitations, a semi-active approach to structural control was formulated. Actuators are no longer used to apply forces to a structure directly. Rather, the forces needed for control are generated indirectly by devices that change the overall damping and stiffness properties of the structure, thereby indirectly removing energy from the system. With small energy consumption characteristics, the semi-active devices are especially attractive solutions for limiting earthquake deflections. Also the amounts of required power for operation are small. (e.g., Lynch and Law 2002, Symans and Constantinou 1999, Preumont and Seto 2008).

In this study the semi-active hydraulic damper (SHD) is applied. The SHD device is a variable damper whose damping coefficient can be changed by changing the orifice opening between the two hydraulic chambers of the damper (e.g., Lynch and Law 2000).

Displacement control criterion is dominant principle in designing of high rise building. In this paper calculated maximum nonlinear displacement from improved capacity demand diagram method suggested by Goel and Chopra (e.g., Chopra and Goel 1999) is used as a control criterion. Remaining structure behavior in the elastic zone is the main subject in this investigation. By using GA and applying optimal control forces based on DPAM, the maximum displacement performance is equated to nonlinear behavior threshold of structure. Assuming, the related deformation to first appeared plastic hinge in columns is defined as nonlinear behavior threshold of structure. The procedure of determining optimal control forces is introduced in the next section.

2. Developed pole assignment method (DPAM)

In designing a linear control system, one of the effective and widely used approaches to find required control force is the pole assignment method (e.g., Xue *et al.* 2007). Let us first consider a structural system whose equation of motion is shown as follows

$$[m]\{\ddot{x}\}+[c]\{\dot{x}\}+[k]\{x\} = -[m]\{l\}\ddot{x}_g-\{u_c\} \tag{1}$$

Where, m, c and k are properties of structure that indicate the matrices of mass, damping and stiffness respectively. The response of structure, $x, \dot{x}$ and $\ddot{x}$ are displacement, velocity and acceleration vector respectively. The system is externally loaded by a dynamic disturbance ($\ddot{x}_g$) and controlled by control forces (u_c). Also l is the unit vector. The equation of motion is shown in the state space form as follows

$$\{\dot{q}\} = [A]\{q\}+\{H\}\ddot{x}_g+[B]\{u_c\} \tag{2}$$

The matrix A is known as the system matrix. The state of the system (q) contains the displacement and velocity response terms of the system. The matrices B and H represent the location of the system actuators and external loads respectively. The parameters of Eq. (2) is introduced as follows

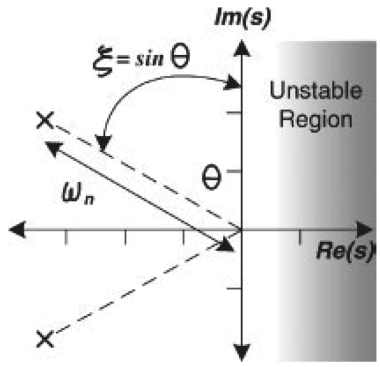

Fig. 2 The relationship between system poles and the corresponding modal frequency and damping ratio

$$[A] = \begin{bmatrix} 0 & I \\ -m^{-1}k & -m^{-1}c \end{bmatrix}, \quad \{q\} = \begin{Bmatrix} x \\ \dot{x} \end{Bmatrix}$$

$$[B] = \begin{bmatrix} 0 \\ -m^{-1} \end{bmatrix}, \quad \{H\} = \begin{Bmatrix} 0 \\ -1 \end{Bmatrix} \tag{3}$$

The eigenvalues of the system matrix (A) characterize the uncontrolled dynamic response of the system. When plotted on the complex plane, these eigenvalues, often termed poles of the system, will all fall in the left half side of the plane if the dynamic system is stable. The right half side of the complex plane represents instability, such that if any system pole is located there, the entire system is dynamically unstable. Graphically, the natural frequency and damping coefficient of each mode of the system can be determined from the location of the poles in the complex plane. The absolute distance from the pole to the origin is the natural frequency of that pole's mode while the sine of the angle between the pole and the positive imaginary axis is the damping ratio of the mode. Fig. 2 depicts the graphical relationship between a system pole and its corresponding modal natural frequency and damping ratio (e.g., Lynch and Law 2002).

To improve the response of a system subjected to external disturbances, the poles of the system can be moved to more desirable locations on the complex plane. Many pole placement techniques exist and can be finding in literature of control (e.g., Amini *et al.* 2005). This paper is an investigation into the development of pole assignment technique that termed developed pole assignment method (DPAM) for application to structural control systems.

Control force vector consists of the gain matrix (F) and the state vector (q) that are considered as follows

$$\{u_c\} = [F]\{q\} \tag{4}$$

The matrix, F is defined by Eq. (5)

$$[F] = [F_k \;\; F_c] \tag{5}$$

The square matrices, F_k and F_c, are type of stiffness and damping property respectively. In this research they are assumed as follows

$$[F_k] = [\beta][k']$$
$$[F_c] = [\alpha][c'] \tag{6}$$

The diagonal matrices, k' and c', Eq. (7), are directly calculated from properties of structure. The matrices β and α, are diagonal coefficient matrices and shown as follows

$$[k'] = \begin{bmatrix} k_1 & \dots & 0 & 0 \\ \vdots & k_2 & & 0 \\ 0 & & \ddots & \vdots \\ 0 & 0 & \dots & k_n \end{bmatrix} \quad [c'] = \begin{bmatrix} C_1 & \dots & 0 & 0 \\ \vdots & C_2 & & 0 \\ 0 & & \ddots & \vdots \\ 0 & 0 & \dots & C_n \end{bmatrix} \tag{7}$$

Where, k_i equal to stiffness of i-th story and C_i is obtained from Eq. (8)

$$C_i = 2\xi\omega_i M_i$$
$$i = 1, 2, \dots, n \qquad n = \text{Number of stories} \tag{8}$$

Where, M_i is i-th element of diagonal mass matrix. The parameters, ξ and ω_i, are damping and i-th mode frequency of structure respectively. Substituting Eq. (4) into Eq. (2), the revised state equation of the system can now be expressed as

$$\{\dot{q}\} = ([A] + [B][F])\{q\} + \{H\}\ddot{x}_g \tag{9}$$

The new system matrix (A_{con}) is obtained by Eq. (10)

$$[A_{con}] = [A] + [B][F] \tag{10}$$

Finally, the equation of the state is changed by substituting Eq. (10) into Eq. (9) as follows

$$\{\dot{q}\} = [A_{con}]\{q\} + \{H\}\ddot{x}_g \tag{11}$$

By using GA and minimizing a target function (defined by Eq. (30)), the coefficient matrices β and α are calculated. Therefore the gain matrix F develops the matrix system, A_{con}, so that performance target is attainable. In fact, the new poles locations are the eigenvalues of the modified system matrix (A_{con}) and performance target of the controlled system. As illustrated in Eq. (4), the calculation of the control forces for the system requires the full state, q, at each time step. In practice, a controller is used to take measurements from the system sensors, assemble the state vector, and calculate the control commands for the control devices.

In this study SHD variable dampers are used as the control devices. The SHD device is a variable damper whose damping coefficient can be changed by changing the orifice opening between the two hydraulic chambers of the damper. In each story the SHD damper is installed. The SHD receives command control force from the processor and calculates the damping coefficient by dividing the command force by the relative velocity between the two floors to which the SHD is installed. The control force is applied if the direction of relative velocity between the two floors is in an opposite direction as the desired control force, else no control force is applied and the damper is set to a default minimum value (e.g., Lynch and Law 2002). Fig. 7 illustrates the installation of the SHD control device and the operational properties of the damper. The stiffness and damping of SHD are coupled with the stiffness and damping of the story as an equivalent dashpot and spring.

3. Performance target of controlled system

In this section, the controlled performance target is determined. At First, capacity and demand diagrams are established to use in improved capacity demand diagram method.

3.1 Capacity diagram

Pushover analysis is applied to determine the capacity diagram. The pushover analysis is performed by subjecting a structure to a monotonically increasing pattern of lateral forces, representing the inertial forces which would be experienced by the structure when subjected to ground shaking. Under incrementally increasing loads various structural elements yield sequentially. Consequently, at each event, the structure experiences a loss in stiffness. Using the pushover analysis, the characteristic nonlinear force - displacement relationship of the MDOF system can be determined. In principle, any force and displacement can be chosen. In this paper, base shear and roof (top) displacement have been used as representative of force and displacement, respectively. The selection of an appropriate lateral load distribution is an important step within the pushover analysis.

In this study, the vector of the lateral loads P used in the pushover analysis is determined as

$$\{P\} = \frac{[m]\{\Phi_1\}}{\{\Phi_1\}^T[m]\{l\}} V \tag{12}$$

Where, V is total base shear. The vector Φ_1 is fundamental (first) mode of structure. Such an approach for the determination of the distribution of lateral loads has a physical background. If the assumed displacement shape was exact and constant during ground shaking, then the distribution of lateral forces would be equal to the distribution of effective earthquake forces. Moreover, by using lateral forces according to Eq. (12), the transformation from the MDOF to the equivalent SDOF system and vice versa follows from simple mathematics (e.g., Fajfar *et al.* 1997). From static it follows

$$F_{in} = F_{out} \tag{13}$$

The internal forces (F_{in}) are equal to the statically applied external loads (F_{out}) which are introduced as

$$F_{in} = [c]\{\dot{x}\} + [k]\{x\}$$
$$F_{out} = \{P\} \tag{14}$$

It will be assumed that the displacement shape Φ_1 is constant, that it does not change during the structural response to ground motion. This is the basic and the most critical assumption. The displacement vector x is defined as

$$\{x\} = \{\Phi_1\}D(t) \tag{15}$$

Where, $D(t)$ is the time dependent top displacement. The effective modal mass for the fundamental vibration mode (M^*) and the modal participation factor (Γ) are defined as follows

$$M^* = \{\Phi_1^T\}[m]\{l\} \qquad \Gamma = \frac{\{\Phi_1^T\}[m]\{l\}}{\{\Phi_1^T\}[m]\{\Phi_1\}} \tag{16}$$

By introducing Eq. (12), (13), (14), and (15) into Eq. (1), and by multiplying from the left side with Φ_1^T, we obtain

$$M^* \frac{\ddot{D}}{\Gamma} + \frac{V}{\Gamma} = -M^* \ddot{x}_g - \{\Phi_1^T\}\{u_c\} \tag{17}$$

If two parameters, D^* and V^*, are introduced as follows

$$D^* = \frac{D}{\Gamma}$$

$$V^* = \frac{V}{\Gamma} \tag{18}$$

Finally, the equation of motion of the equivalent SDOF system can be written as

$$M^* \ddot{D}^* + V^* = -M^* \ddot{x}_g - \{\Phi_1^T\}\{u_c\} \tag{19}$$

Note that the constant Γ applies for the transformation of both displacements and forces. As a consequence, the force - displacement relationship (the V-D diagram) determined for the MDOF system (Result of pushover analysis) applies also to the equivalent SDOF system (the $V^* - D^*$ diagram), provided that both force and displacement are divided by Γ. This can be visualized by changing the scale on both axes of the force - displacement diagram (Fig. 3). The initial stiffness of the equivalent SDOF system remains the same as that defined by the base shear - top displacement diagram of the MDOF system. In order to determine a simplified (elastic - perfectly plastic) force – displacement relationship for the equivalent SDOF system, engineering judgment has to be used (e.g., Fajfar *et al.* 1997). The capacity curve in improved capacity demand diagram method is used in acceleration – displacement (A-D) Format. By dividing V^* with M^*, the acceleration is obtained.

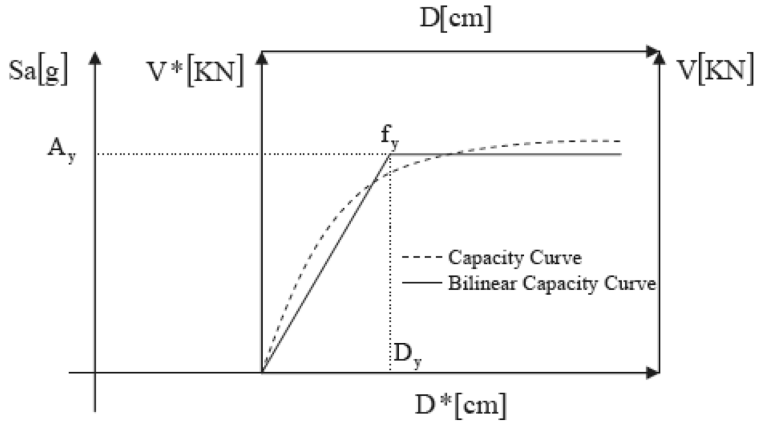

Fig. 3 Pushover curve and the corresponding capacity diagram. Note the different scales. The top displacement, *D*, and the base shear, *V*, apply to MDOF system, whereas the force V^* and the displacement D^* apply to the equivalent SDOF system. The acceleration, *Sa*, belongs to the capacity diagram in A-D Format

3.2 Demand diagram

The improved capacity demand diagram method uses the well known constant ductility design spectrum for the demand diagram, instead of the elastic design spectrum for equivalent linear systems in ATC-40 procedures. A constant ductility design spectrum is established by reducing the elastic design spectrum by appropriate ductility dependent factors that depend on natural vibration period (T_n).

The right side of Eq. (19) can be considered as improved earthquake force for equivalent SDOF system. By introducing $\ddot{X}_g$ as decreased ground acceleration recorded of specified earthquake, it is obtained as follows

$$\ddot{X}_g = \ddot{x}_g + \frac{\{\Phi_1^T\}\{u_c\}}{M^*} \tag{20}$$

The peak ground acceleration (PGA) is defined from $\ddot{X}_g$. By using sequence integrating from $\ddot{X}_g$, the decreased ground velocity and displacement are obtained. Consequently, the peak ground velocity (PGV) and the peak ground displacement (PGD) are determined. The demand curve, applied in the improved capacity demand diagram method, can be constructed based on decreased PGA, PGV and PGD.

3.3 Displacement performance

The yield strength f_y of each elastoplastic system analyzed was chosen corresponding to an allowable ductility μ

$$f_y = \left(\frac{A_y}{g}\right)w \tag{21}$$

Where, w and g are weight of the system and acceleration due to gravity respectively. Also A_y is the pseudo acceleration corresponding to the allowable ductility and the vibration properties, natural period T_n and damping ratio ξ, of the system in its linear range of vibration. According to Fig. 3, the pseudo acceleration A_y related to the yield strength and the yield deformation D_Y is determined. Elastic vibration period T_n is obtained as follows

$$T_n = 2\pi\sqrt{\frac{D_y}{A_y}} \tag{22}$$

The yield strength reduction factor is given by

$$R_y = \frac{f_0}{f_y} = \frac{A}{A_y} \tag{23}$$

Where, f_0 is the minimum yield strength required for the structure to remain elastic, obtained as follows

$$f_0 = \left(\frac{A}{g}\right)w \tag{24}$$

Also, A is the pseudo acceleration ordinate of the elastic design spectrum, constructed based on decreased ground acceleration recorded at (T_n, ξ). The suggested elastic design spectrum (Fig. 4) is

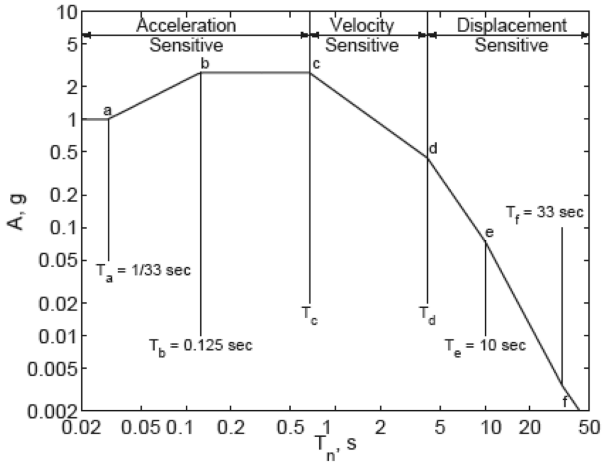

Fig. 4 Newmark-Hall elastic design spectrum

the median plus one standard deviation spectrum constructed by the procedures of Newmark and Hall, as described by Chopra (e.g., Chopra 1995).

For determining μ the $R_y - \mu - T_n$ equations for elastoplastic systems, consistent with the Newmark-Hall inelastic design spectra are used in this paper

$$\mu = \begin{cases} \text{Undefined} & T_n < T_a \\ \dfrac{1+R_y^{2/\beta}}{2} & T_a < T_n < T_b \\ \dfrac{1+R_y^2}{2} & T_b < T_n < T_{c'} \\ \dfrac{T_c}{T_n} R_y & T_{c'} < T_n < T_c \\ R_y & T_n > T_c \end{cases} \tag{25}$$

The parameter β is calculated as follows

$$\beta = \ln\frac{T_1}{T_a} / \ln\frac{T_b}{T_a} \tag{26}$$

And the T_a, T_b and T_c are defined in Fig. 4 and $T_{c'}$ is the period where the constant A and constant V (pseudo velocity) branches of the inelastic design spectrum intersect. For a given R_y, ductility factor μ can be calculated for all T_n except for $T_b < T_n < T_c$, wherein two possibilities need to be checked since $T_{c'}$ itself depends on μ. Assuming that $T_b < T_n < T_{c'}$, according to Eq. (25) μ is calculated. For this value of μ, $T_{c'}$ is obtained as follows

$$T_c' = \frac{T_c\sqrt{2\mu - 1}}{\mu} \tag{27}$$

If $T_c' > T_n$ clearly the assumption that $T_b < T_n < T_{c'}$ is correct, else the assumption $T_{c'} < T_n < T_c$ is correct.

The maximum nonlinear dynamic deformation D^* of SDOF system is obtained as follows

$$D^* = \mu \times R_y \tag{28}$$

Using Eq. (18), the maximum nonlinear dynamic deformation of MDOF system is determined as follows

$$D = \Gamma \times D^* \tag{29}$$

Where, D is performance target of MDOF system. Therefore the gain matrix F in the DPAM develops the matrix system A_{con} so that, target displacement performance is equated to D.

4. Target function

The target function considered here is introduced as follows

$$\text{Target function} = \left|\Delta_{roof} - \Delta_{Plastic}\right| \tag{30}$$

Where Δ_{Roof} is the nonlinear dynamic deformation of MDOF system (D) which was determined in previous section. The displacement related to the first appeared plastic hinge in the columns is defined by $\Delta_{Plastic}$ which is determined using pushover analysis. The number of variables in the target function is equal to $2n$, which is also the number of variables related to the elements of diagonal coefficient matrices β and α. Minimizing the target function using the GA yields the optimum values of matrices β and α. Allocating of proportion is restricted to a condition, in which if any changes occur in proportion of each element of diagonal coefficient matrices then the disturbance will be found in system behavior. Based on this solution, properties of structure, stiffness and damping of stories are changed optimally without any disturbances in system behavior. This is an optimal solution in the multi objective optimization sense.

Based on the optimal distribution of coefficient matrices, the optimal location and the number of actuators are determined. It means that under a specified earthquake, if there is no need to install actuator in i-th story of the structure and the DPAM gives the coefficients β_i and α_i approximately zero.

The computational steps of DPAM based on the improved capacity demand diagram are shown in Fig. 5 and summarized as follows:

1) By the help of sensors the feedback of input and output data are obtained.
2) The coefficient matrices β and α are guessed by GA.
3) By determining β and α, the gain matrix, F, is obtained using Eqs. (5) and (6). Also the control forces are determined by the help of Eq. (4).
4) The equivalent SDOF system can be constructed from Eq. (19).
5) Using Eq. (20), the ground acceleration is developed.
6) Pushover analysis is applied to determine capacity diagram.
7) From Eq. (25) the inelastic design spectra based on improved ground acceleration is generated.
8) The maximum nonlinear dynamic deformation D^* of SDOF system is obtained using Eq. (28).
9) The maximum nonlinear dynamic deformation of MDOF system is obtained from Eq. (29).
10) If the absolute value of target function is close to zero (for example smaller than 0.05) then the procedure is completed, else the GA reproduces the better coefficient matrices and the procedure is repeated until the absolute value of target function goes to zero.

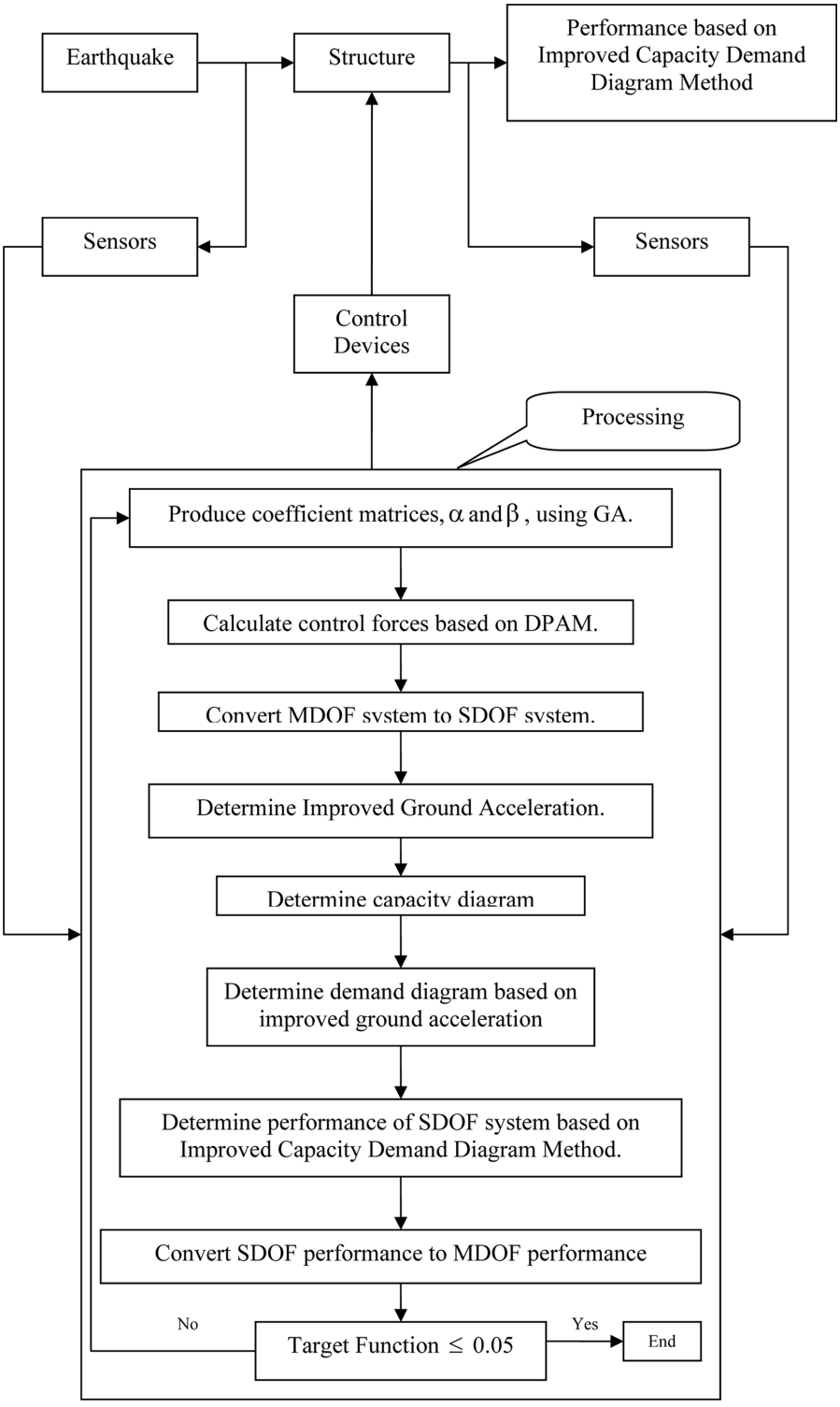

Fig. 5 The algorithm of control based on displacement performance

5. Linear quadratic regulation (LQR)

The LQR method is applied in this study for comparison and verification. In designing a linear control system, one of the most effective and widely used approaches is the LQR. The LQR approach is briefly reviewed (e.g., Lynch and Law 2002). The LQR has emerged as a reliable systematic guide to pole placement that allows for the weighting of control response against control effort. The LQR method provides an optimal control solution through the minimization of a cost function that encapsulates the system's control objectives.

$$J = \int_0^\infty (q^T Q q + u_c^T R u_c) dt \tag{31}$$

The cost function, J, contains two control objectives; the minimization of structural response, q, and the minimization of the input control forces, u_c, required to attain those responses with a weighting matrices, R and Q, which is included to vary the proportional emphasis between the two terms.

The result of the minimization of the cost function is a static gain matrix, F, that when multiplied by the full state of the system q yields the optimal control force vector.

$$u_c = -R^{-1} B^T Z q = -F q \tag{32}$$

The Ricatti matrix, Z, represents the solution of the algebraic Ricatti equation that results in the minimization procedure.

$$ZA + A^T Z + Q - ZBR^{-1} B^T Z = 0 \tag{33}$$

The new pole locations of the closed loop system are the eigenvalues of the modified system matrix A_{con}. Key to understanding the location of the closed loop poles is the understanding of the influence of the individual terms of the LQR cost function. If Q emphasizes on the vector of displacements of the system nodes, the poles will migrate in a manner consistent to increased system stiffness. Increased system stiffness is synonymous with poles migrating outward as shown in Fig. 6(a). On the other hand, if the emphasized response is system velocities, the resulting control solution will cause poles to migrate consistent with increased system damping. Pole rotating about the origin towards the negative real axis is consistent with increased system damping, as shown in Fig. 6(b). A combination of displacement and velocity in the emphasized response would result in a pole migration pattern that would be influenced by both increased system stiffness and damping. How far the final poles result on these generalized trajectory paths is dependent upon the weighting matrix R. If R is near infinity, the poles will not move since this makes control effort expensive. As R decreases towards zero, control becomes inexpensive and poles result in positions far from their open loop positions.

The limitations of the LQR controller should be noted. In particular, the optimality of the LQR solution is dependent upon the assumption of a linear system. Application in structures excited by large seismic events, the assumption of system linearity is invalid. For use in nonlinear systems, the nonlinearity of the structure has to be modeled in the analysis and an additional control loop is designed for the control system that cancels the system nonlinearities. Another inherent weakness of the LQR method is its heavy dependence upon the assumption of perfect knowledge of the system.

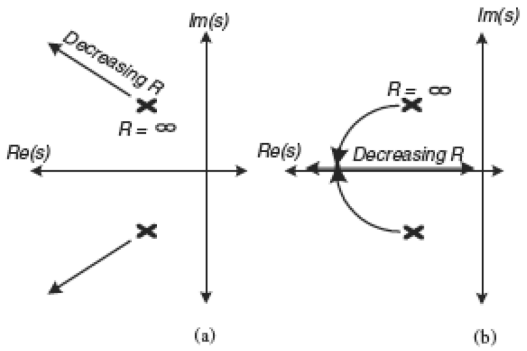

Fig. 6 Influence of the system cost function on closed loop pole locations

If the model used in the design of the controller is incorrect, the LQR solution is no longer optimal and could even be destabilizing (e.g., Lynch and Law 2002).

6. Stability of the control solution

Stability is defined by a system's tendency to grow or decay in response to an input disturbance to the system. If the response decays, the system is considered stable. However, if the response grows in time, then the system is defined as unstable. The stability of a dynamic system is characterized by the location of the system poles in the complex plane. Given the existence of at least one pole in the right half part of the complex plane, the system is considered unstable and will exhibit growing system response to input disturbances. If all poles are located in the left half part of the complex plane, the system is stable. Various tests for linear system stability exist such as the Routh's stability criterion and the Nyquist stability criterion (e.g., Franklin *et al.* 1994).

For the LQR controller, closed loop system stability is guaranteed if two criteria are met: (a) if the system matrix, A, and the control location matrix, Bu, of Eq. (2) are a controllable pair; and (b) R and Q of Eq. (37) are both positive definite (e.g., Stengel 1994). The controllability criterion ensures that the controller has influence on all modes, particularly unstable modes, of the system. The positive definite criteria on R allows for control effort to have a positive effect on the cost function, J, while the positive definite criterion on Q provides penalty on system responses, particularly unstable responses.

Unlike the LQR controller, the current controller derived in the DPAM has not been shown to be mathematically stable in closed form. Further work is needed to consider the limitations of the controller with regard to stability concerns. However, when at the first we consider the restriction, remaining structure behavior in elastic zone, the stability of the structure is observed.

7. Numerical example: 30-story steel

To illustrate the efficiency of DPAM, a hypothetical 30-story 2-dimentional steel moment frame structure is used. Also a set of 30 SHD dampers is distributed throughout the structure. In each story only one SHD damper is considered. Fig. 7 illustrates the SHM properties, the 30-story steel

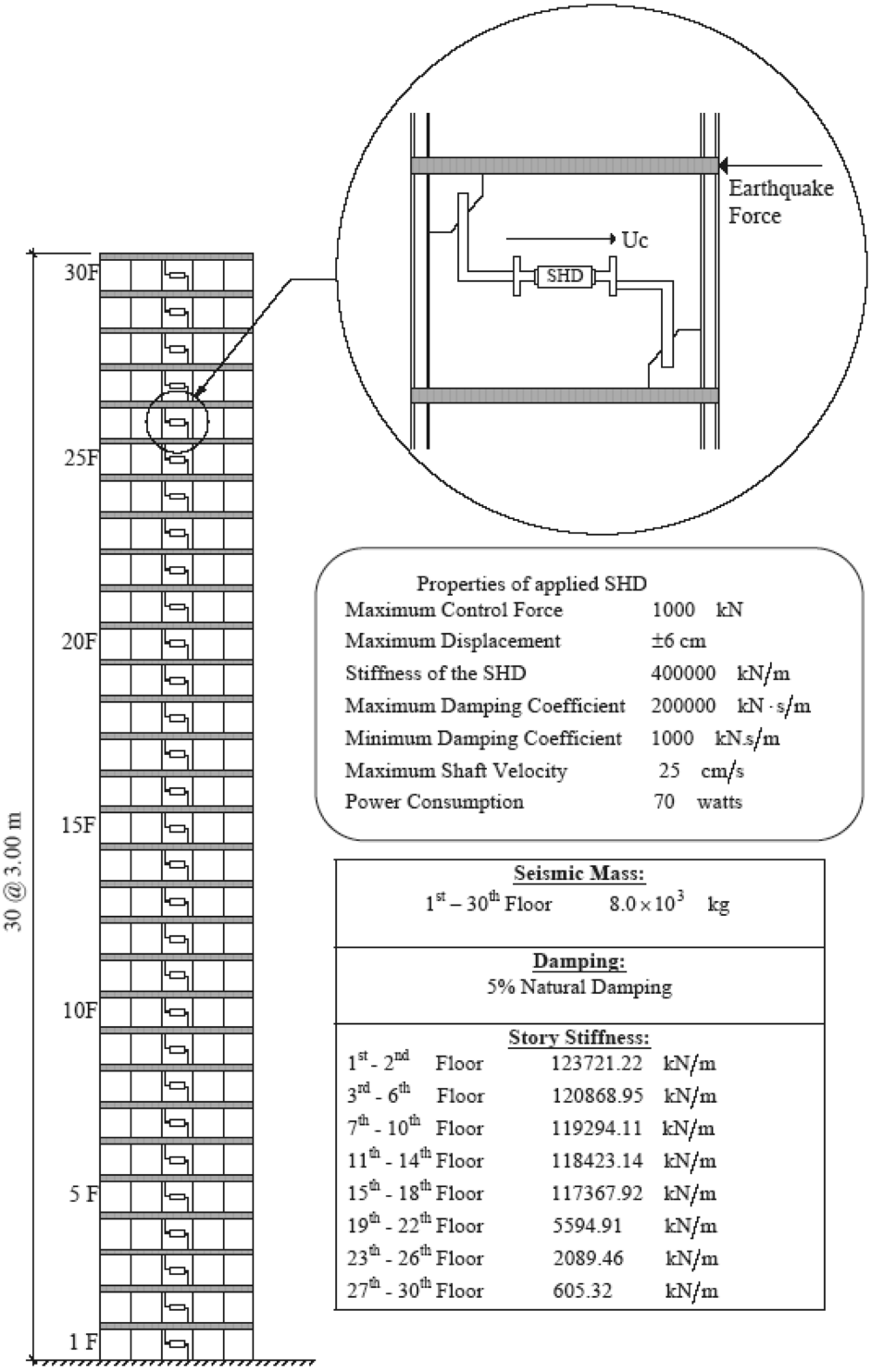

Properties of applied SHD		
Maximum Control Force	1000	kN
Maximum Displacement	±6 cm	
Stiffness of the SHD	400000	kN/m
Maximum Damping Coefficient	200000	kN · s/m
Minimum Damping Coefficient	1000	kN.s/m
Maximum Shaft Velocity	25	cm/s
Power Consumption	70	watts

Seismic Mass:

$1^{st} - 30^{th}$ Floor 8.0×10^3 kg

Damping:

5% Natural Damping

Story Stiffness:

1^{st} - 2^{nd} Floor	123721.22	kN/m
3^{rd} - 6^{th} Floor	120868.95	kN/m
7^{th} - 10^{th} Floor	119294.11	kN/m
11^{th} - 14^{th} Floor	118423.14	kN/m
15^{th} - 18^{th} Floor	117367.92	kN/m
19^{th} - 22^{th} Floor	5594.91	kN/m
23^{th} - 26^{th} Floor	2089.46	kN/m
27^{th} - 30^{th} Floor	605.32	kN/m

Fig. 7 Properties of 30-story steel moment frame structure and SHD device

moment frame structure and its stories stiffness as well as damping. Maximum control force is obtained by SHM through constrain value for that. Tables 3 and 4 show the modal participating mass ratio for the first three modes of finite element model and lumped mass model of the system, respectively, in x direction (Ux). It is clear that the first mode is the fundamental mode for the two models. Hence to simplify the analysis, the structure is modeled as a lumped mass shear model. To determine the optimal control forces during induced earthquake by using DPAM controller, the processor sends commands to control devices such as SHD to produce the needed control forces. During the earthquake, the total power consumption is calculated based on the properties of SHD device. Note that our main goal is keeping the structure behavior in the elastic zone. To evaluate the efficiency of the DPAM strategy and in order to considering the different intensity and duration in earthquake records, three far field earthquake records such as El Centro (1940 NS), Tabas (1987 NS) and Kobe (1995 NS) are used. The peak ground velocity of the three earthquake records are 36.15, 126.48, and 81.30 cm/sec, respectively. Also the peak ground accelerations of them are 0.318 g, 0.933 g, and 0.821 g, respectively. The acceleration response spectra of the input earthquakes are shown in Fig. 8.

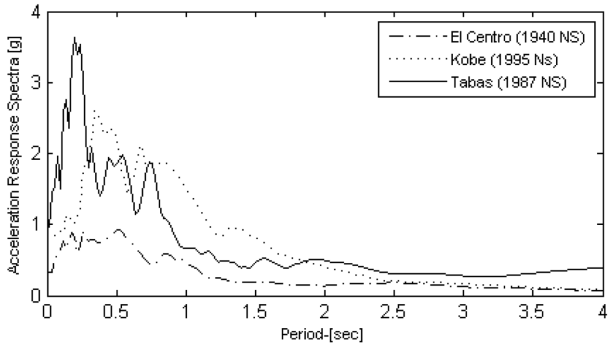

Fig. 8 Acceleration response spectra of the seismic disturbances used (damping ratio 5%)

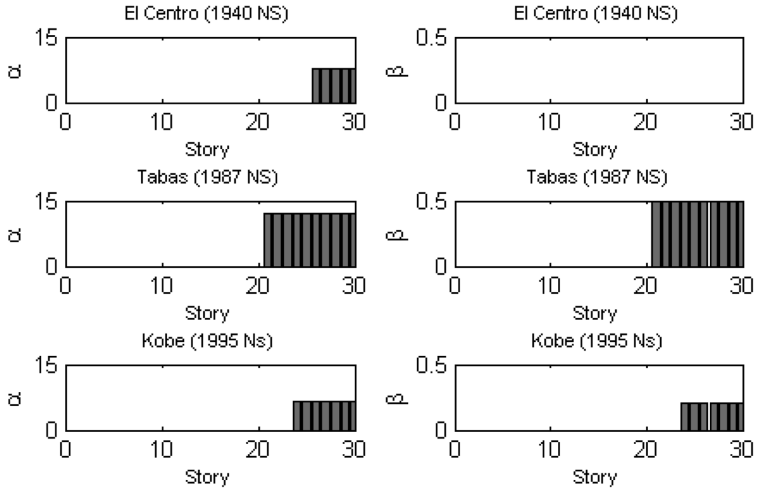

Fig. 9 Result of GA optimization for coefficient matrices based on DPAM in 30-Story steel structure

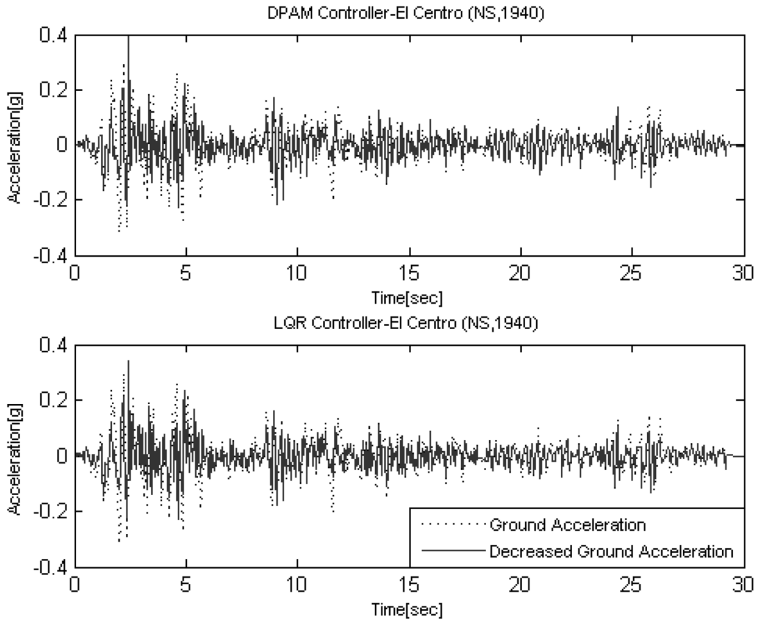

Fig. 10 Decreased ground acceleration – El Centro (1940, NS)

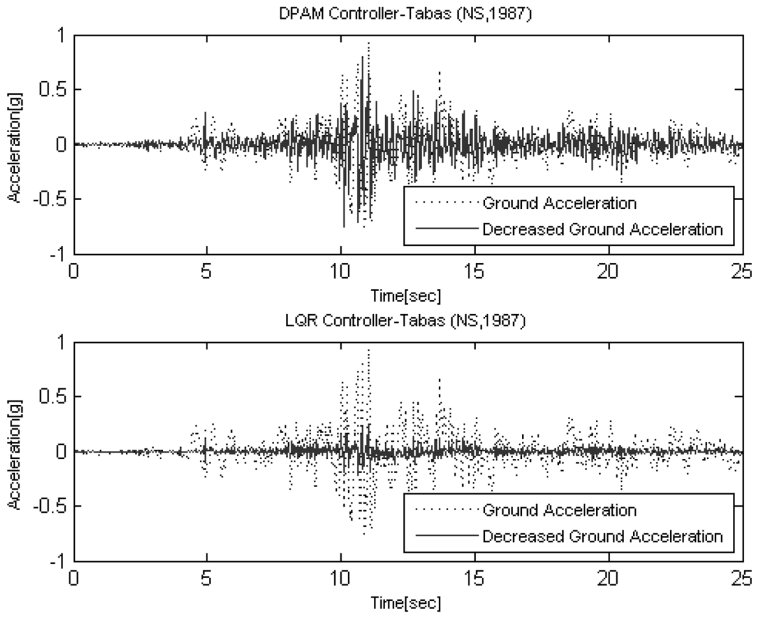

Fig. 11 Decreased ground acceleration – Tabas (1987, NS)

Using pushover analyses the obtained displacement related to the first appeared plastic hinge in columns, $\Delta_{Plastic}$, is equal to 10.20 cm. In presence of the three above mentioned earthquakes, the improved capacity demand diagram method estimates the maximum nonlinear dynamic deformation of the structure as 13.74, 48.06, and 30.89 cm, respectively. Therefore, the structure behavior passes

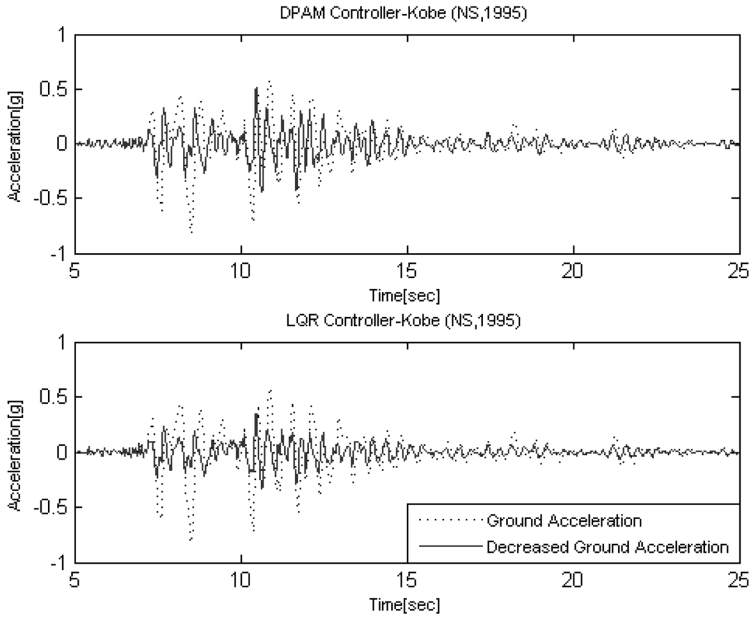

Fig. 12 Decreased ground acceleration – Kobe (1995, NS)

Table 1 The weighting matrices, Q and R, based on LQR Method, in 30-Story steel structure

Earthquake	Q	R
El Centro (NS, 1940)	$Q = [I]_{60\times60}$	$6.6990\text{E-}011\times[I]_{30\times30}$
Tabas (NS, 1987)		$4.8000\text{E-}013\times[I]_{30\times30}$
Kobe (NS, 1995)		$2.4700\text{E-}011\times[I]_{30\times30}$

through the elastic zone to the plastic area. So, the control forces are needed to keep the structure in its elastic capacity. Two controllers containing DPAM and LQR are used to reduce the response of structure and their results are compared.

By minimizing the target function (defined by Eq. (30)) using GA, the optimum values of matrices β and α are determined. Fig. 9 illustrates the result of GA optimization for coefficient matrices. As mentioned before, based on the optimal distribution of coefficient matrices, the optimal location and the number of actuators are determined. The numbers of used SHM devices in three earthquakes are 5, 10 and 7 respectively as shown in Fig. 9. In the presence of applied control forces, the ground accelerations are decreased as shown in Figs. 10, 11, and 12. The demand curves based on decreased ground accelerations is used in improved capacity demand diagram method. Also the performance of the structure is equated to the threshold of nonlinear behavior of structure. To design the LQR controller, the weighting matrix on state response, Q, is selected with the objective of reducing system velocity and displacement responses. The weighting on control, R, is increased up to a point of actuation saturation. The summary of results containing the weighting matrices in the LQR method is given by Table 1. The results of total power consumption and number of necessary SHD devices in the two above mentioned methods are compared in Table 2. It shows that the total power consumption and number of SHD devices, during the induced

Table 2 Performance comparison of two controllers, DPAM and LQR, in 30-Story steel structure

Earthquake	Controller	Number of control device	Maximum control force [KN]	Percentage of maximum control force based on total weight of structure	Total power [KW]
El Centro (NS, 1940)	DPAM	5	78.25	3.22	2.58
	LQR	30	23.83	0.99	3.54
Kobe (NS, 1995)	DPAM	7	158.96	6.62	6.36
	LQR	30	72.66	3.03	7.69
Tabas (NS, 1987)	DPAM	10	486.67	20.27	12.10
	LQR	30	84.53	3.52	19.21

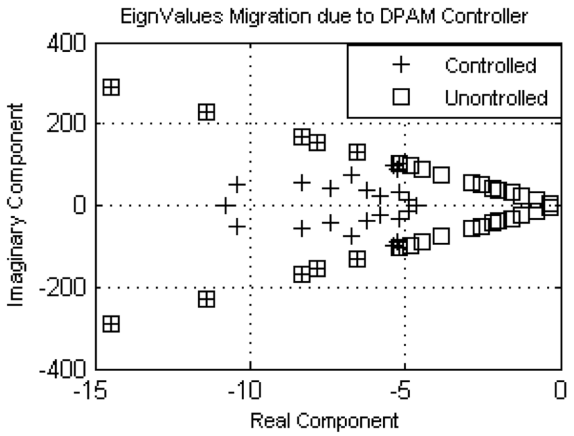

Fig. 13 The migration of system eigenvalues due to DPAM controllers – El Centro (1940, NS)

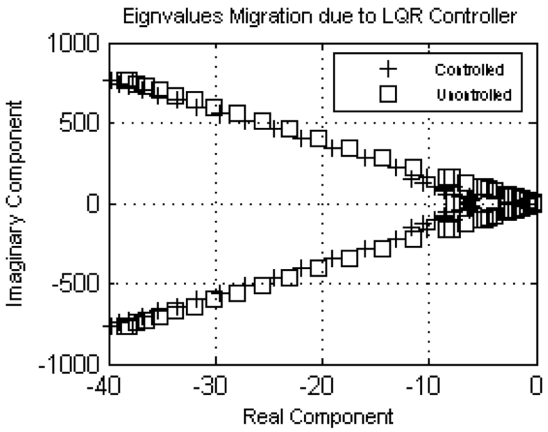

Fig. 14 The migration of system eigenvalues due to LQR controllers – El Centro (1940, NS)

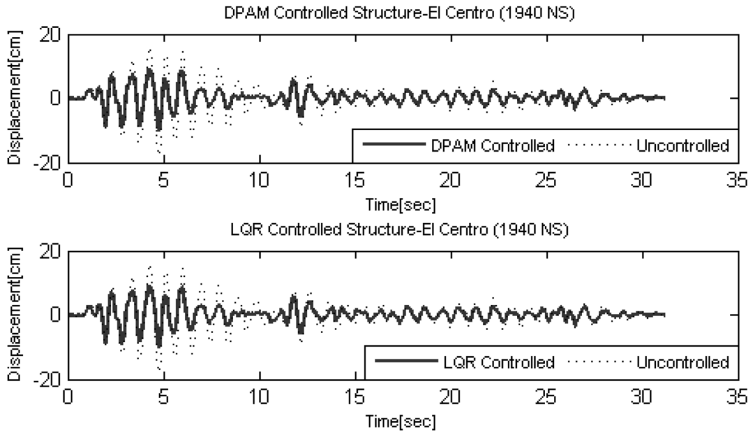

Fig. 15 Time history response of controlled 30-story structure due to El Centro (NS, 1940)

Table 3 Modal participating mass ratio of finite element model

Mode	Period (Sec)	UX (%)	SumUX (%)
1	5.27	77.51	77.51
2	1.40	11.05	88.56
3	0.58	4.24	92.80

Table 4 Modal participating mass ratio of lumped mass model

Mode	Period (Sec)	UX (%)	SumUX (%)
1	0.43	97.52	97.52
2	0.21	0.96	98.48
3	0.11	1.35	99.82

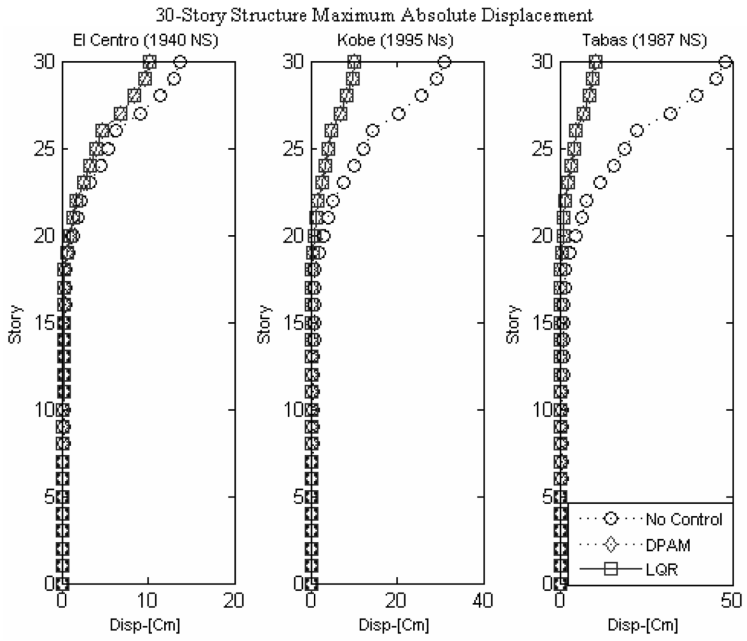

Fig. 16 Control applied to the 30-story structure—LQR versus DPAM-displacements

earthquakes, in DPAM are less than LQR method.

The poles migration to left side of complex area is shown in Figs. 13 and 14. They clear that the system is more stable than initial conditions and there isn't any disturbances in system behavior. Fig. 15 shows the time history response of the controlled structure subjected to the El Centro earthquake. The simplified nonlinear analysis approximately gives the same result in comparison with the time history analysis.

Figs. 16 and 17 present the reduction of both maximum absolute displacements and maximum inter story drifts. These are quite significant for the both of LQR and DPAM controllers in

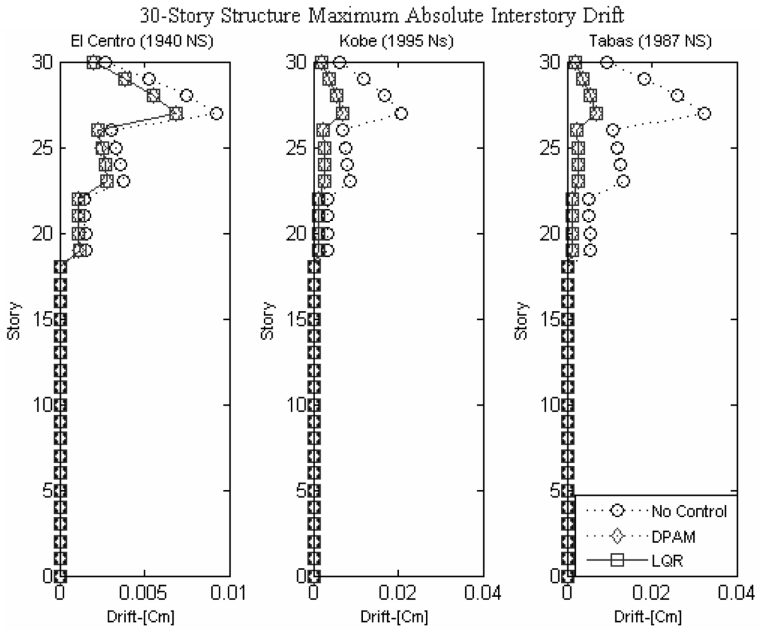

Fig. 17 Control applied to the 30-story structure—LQR versus DPAM-drifts

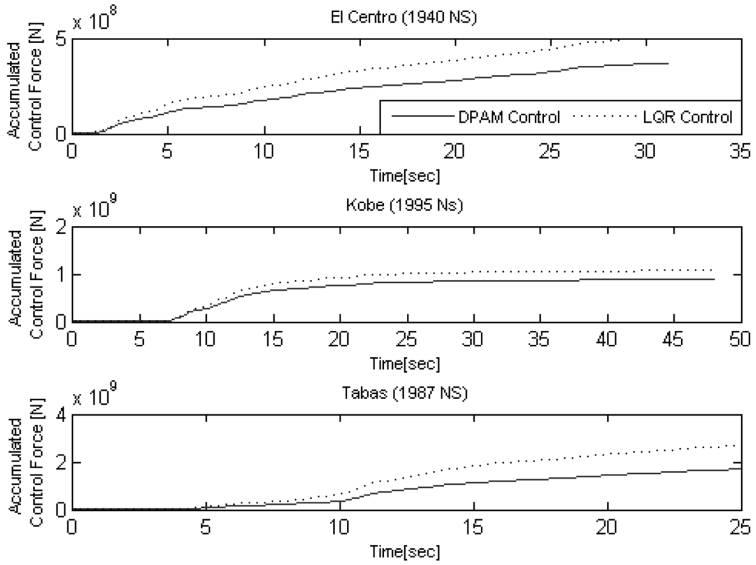

Fig. 18 Accumulated control effort of 30-story structure using LQR and DPAM controllers

comparison with the uncontrolled response. If we compare the performance of the DPAM and LQR controllers with each other, it can be safely concluded that both of them yield similar reductions of structural response.

The total control effort of the control system is considered to ensure that the DPAM controller is not using excessive amounts of control energy to remain competitive with the LQR solution. As

seen in Fig. 18, during the three seismic disturbances the DPAM controller is using control effort approximately 36.21%, 58.79%, and 13.10%, respectively, less than the LQR controller.

8. Conclusions

While nonlinear response history analysis is the most rigorous procedure to compute seismic demands, simplified nonlinear analysis procedures are applied to determine the displacement demand imposed on a building expected to deform inelastically. Here for the first time, the improved capacity demand diagram method in control of the structural system is applied. We presented the formulation and implementation of the developed pole assignment method in control of structural systems. It was shown that the control technique can successfully limit the response of structures during the large seismic events. By applying the control forces, the ground acceleration is decreased. Based on this reduction, displacement performance of structure due to decreased ground acceleration is equated to the threshold of nonlinear behavior of structure. Using the optimal control forces, the structure responses are reduced. Also the system becomes more stable than uncontrolled system condition. There is no any disturbance in system behavior and the structure is forced to behave in linear zone of capacity diagram. The system matrix in DPAM is modified. In this case, changing modal damping and natural frequencies of structure adapts response of structure to performance target.

In comparison to the widely used LQR controller, it was shown that the proposed method is more effective. Based on optimal distribution of coefficient matrices, optimal location and number of actuators are determined. In DPAM the total consumed power of control devices is considerably less than the LQR method.

References

Amini, F. and Vahdani, R. (2008), "Fuzzy optimal control of uncertain dynamic characteristics in tall buildings subjected to seismic excitation", *Int. JVC.*, **14**(12), 1843-1867.

Amini, F., Vahdani, R. and Rahemi, B. (2005), "Semi-active control of variable stiffness and damping systems by the pole-assignment method", *Proceedings of '12 CMEM Structures Congress*, Malta.

ATC (1996), *Seismic Evaluation and Retrofit of Concrete Buildings*, Rep. ATC-40, Applied Technology Council, Redwood City, Calif.

Bertero, V.V. (1995), *Tri-service Manual Methods. In Performance-based Seismic Engineering of Buildings,* Sacramento, Structural Engineers Assn. of California, Calif.

Casarotti, C. and Pinho, R. (2007), "An adaptive capacity spectrum method for assessment of bridges subjected to earthquake action", *Int. J. Bull. Earthq. Eng.*, **5**, 377-390.

Chopra, A.K. (1995), *Dynamics of Structures: Theory and Applications to Earthquake Engineering*, Prentice Hall, Englewood Cliffs, NJ.

Chopra, A.K. and Goel, R.K. (1999), "Capacity-demand-diagram methods for estimating seismic deformation of inelastic structures: SDF systems", *Int. J. Report PEER.*, University of California, Berkeley, CA.

Chopra, A.K. and Goel, R.K. (2002), "A modal pushover analysis procedure for estimating seismic demands for buildings", *Int. J. Earthq. Eng. Struct. D.*, **31**, 561-582.

Fajfar, P., Gaspersic, P. and Drobnic, D. (1997), "A simplified nonlinear method for seismic damage analysis of structures", *Proceedings of the Workshop on Seismic Design Methodologies for the Next Generation of Codes*, Rotterdam.

Fajfar, P. (1999) "Capacity spectrum method based on inelastic demand spectra", *Int. J. Earthq. Eng. Struct. D.,* **28**, 979-993.
FEMA (1997), *NEHRP Commentary on the Guidelines for the Seismic Rehabilitation of Buildings*, FEMA-274, Federal Emergency Management Agency, Washington, D.C.
Franklin, G., Powell, J. and Emami-Naeini, A. (1994), *Feedback Control of Dynamic Systems*, Addison-Wesley Publishing Company, MA.
Freeman, S.A., Nicoletti, J.P. and Tyrell, J.V. (1975), "Evaluations of existing buildings for seismic risk-a case study of Puget Sound Naval Shipyard Bremerton, Washington", *Proceedings of the 1st US National Conference on Earthquake Engineering*, Oakland, California.
Freeman, S.A. (1978), "Prediction of response of concrete buildings to severe earthquake motion", *Publ. Am. Concrete Institute, Detroit*, **55**, 589-605.
Freeman, S.A. (2004), "Review of the development of the capacity spectrum method", *ISET. Earthq. Technol.*, **438**(41), 1-13.
Lee, D.G., Choi, W.H., Cheong, M.C. and Kim, D.K. (2006), "Evaluation of seismic performance of multistory building structures based on the equivalent responses", *Int. J. Eng. Struct.,* **28**, 837-856.
Lynch, J. and Law, K. (2000), "A market-based control solution for semi-active structural control", *Proceedings of the Eight International Conference*, Stanford, CA, USA.
Lynch, J. and Law, K. (2002), "Market-based control of linear structural systems", *Int. J. Earthq. Eng. Struct. D.*, **31**, 1855-1877.
Lynch, J. and Law, K. (2002), "Energy market-based control of linear civil structures", *Proceedings of the US-Korea Workshop on Smart Structural Systems*, Pusan, Korea.
Preumont, A. and Seto, K. (2008), *Active Control of Structures*, John Wiley & Sons Ltd.
Reinhorn, A.M. (1997), "Inelastic analysis techniques in seismic evaluations", *Proceedings of the Workshop on Seismic Design Methodologies for the Next Generation of Codes*, Rotterdam.
Stengel, R. (1994), *Optimal Control and Estimation*, Dover Publications, New York.
Symans, M.D. and Constantinou, M.C. (1999), "Semi-active control systems for seismic protection of structures: a state-of-the-art review", *Int. J. Eng. Struct.*, **21**(6), 469-487.
Xue, D., Chen, Y.Q. and Atherton, D.P. (2007), *Linear Feedback Control Analysis and Design with MATLAB*, Society for Industrial and Applied Mathematics.
Xue, Q. (2001), "A direct displacement-based seismic design procedure of inelastic structures", *Int. J. Eng. Struct.,* **23**, 1453-1460.
Xue, Q. and Chen, C.C. (2003), "Performance-based seismic design of structures: a direct displacement-based approach", *Int. J. Eng. Struct.,* **25**, 1803-1813.